RSC Advances

ROYAL SOCIETY OF CHEMISTRY

www.rsc.org/advances

RSC Advances

RSCPublishing

COMMUNICATION

Lysosome-Specific One-Photon Fluorescence Staining and Two-Photon Singlet Oxygen Generation by Molecular Dyad

Cite this: DOI: 10.1039/x0xx00000x

Received ooth January 2012,
Accepted ooth January 2012

DOI: 10.1039/x0xx00000x

www.rsc.org/

Somin Cho,[a] Youngmin You,[b,*] and Wonwoo Nam[a,*]

A dual functional molecular dyad, consisting of a cyclometalated Ir(III) complex and rhodamine B, has been synthesized and evaluated for its ability for independent operations of fluorescence staining and photodynamic therapy.

Image-guided photodynamic therapy holds considerable promise as a reliable strategy to treat cancer because the technique can avoid undesired photodamage.[1-4] Dual functional molecules that produce photoluminescence and reactive oxygen species under photoirradiation are prerequisite for the operation of the image-guided photodynamic therapy. Although phosphorescent transition metal complexes, such as those containing Ru(II),[5-8] Ir(III),[9, 10] and Pt(II),[11] have been demonstrated for the dual function, their practicability is limited because singlet oxygen ($^1O_2$) produced during phosphorescence imaging provokes deleterious effects. Thus, the development of molecules with controllable phototoxicity remains a significant challenge, requiring the judicious molecular design that allows for independent operations of the imaging and photosensitization of $^1O_2$. Specifically, utility of modulating function by selecting the photoirradiation wavelength is urgently required.

To address this challenge, we designed and synthesized a molecular dyad comprising a biscyclometalated Ir(III) complex and rhodamine B (RhB). In this dyad structure, the former sensitizes $^1O_2$ under two-photon irradiation at 800 nm, while the latter produces strong red fluorescence under one-photon irradiation at 550 nm. Notably, the two photofunctions can be operated in a fully independent manner because the electronic spin selection rule effectively prevents the bidirectional energy transfer between the molecular entities. The unique spin-gated energy transfer has been proved by steady-state and transient photoluminescence studies. Finally, photobiological utility of the dyad has been fully evaluated in vitro. It should be noted that this is the first report on the single molecule containing an Ir(III) complex capable of independent operation of fluorescence imaging and $^1O_2$ sensitization for potential applications in image-guided photodynamic therapy.

The dyad (Irbtp–RhB) was prepared by forming a thiourea linkage between an amine-functionalized Ir(III) complex (Irbtp)[12] and rhodamine B isothiocyanate (RhB-NCS) in the presence of triethylamine (Scheme 1). Structures and purity of Irbtp–RhB and its precursors were examined by standard characterization methods, and the spectral identification data fully agreed with the proposed structure (Electronic Supplementary Information, ESI†). UV–vis absorption spectrum of a deaerated acetonitrile solution of 10 μM Irbtp–RhB is a simple superposition of the absorption spectra of the individual components of Irbtp and RhB (Fig. 1), excluding any ground-state interaction between two units. The dyad exhibits strong red fluorescence (λ_{em} = 570 nm, photoluminescence lifetime (τ_{obs}) = 1.84 ns, photoluminescence quantum yield (Φ_{PL}) = 2.3±0.2%) upon photoexcitation of the RhB moiety (λ_{ex} = 490–550 nm), whereas weaker phosphorescence from Irbtp (λ_{em} = 592 nm, τ_{obs} = 1.68 μs, Φ_{PL} = 1.2±0.1%) with a characteristic vibronic progression of $\Delta\nu$ = 1340 cm^{-1} is observed when the photoexcitation beam at λ_{ex} = 330–450 nm is provided (Fig. 1).[12, 13] The photoluminescence excitation spectrum (PLE) for the 570 nm emission overlaps exclusively with the absorption band of the RhB unit (Fig. 1b), supporting that the fluorescence emission is due to selective photoexcitation of RhB. The minimal contribution of the Irbtp unit

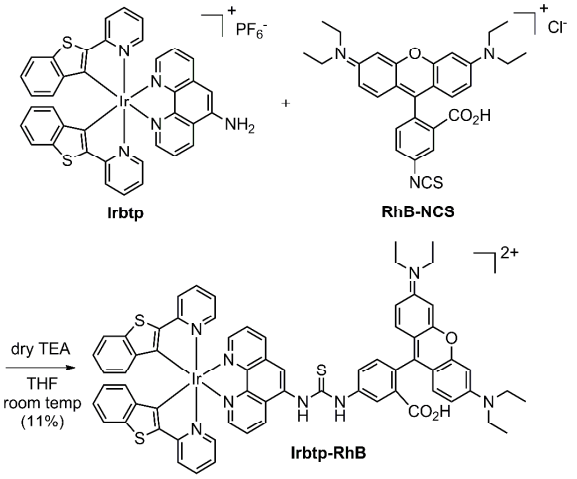

Scheme 1 Synthesis of Irbtp–RhB

to the PLE spectrum precludes occurrence of singlet–singlet energy transfer from Irbtp to RhB. In addition, spin-restricted energy transfer from the singlet excited state of the RhB unit to the triplet state of the Irbtp unit is also ruled out, because the fluorescence lifetimes for the RhB fluorescence of Irbtp–RhB and RhB–NCS are identical (ESI†, Fig. S1).

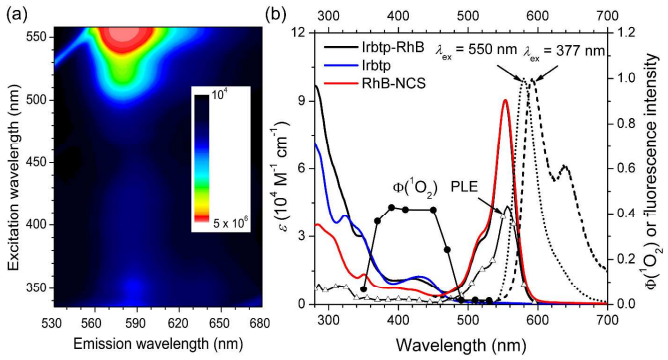

Fig. 1 Spectral properties of 10 μM Irbtp–RhB in deaerated acetonitrile. (a) Contour plot of photoluminescence intensities obtained with varying the excitation (330–560 nm) and emission (530–680 nm) wavelengths. (b) UV–vis absorption spectra (solid lines) of acetonitrile solutions of 10 μM Irbtp–RhB (black), 10 μM Irbtp (blue), and 10 μM RhB–NCS (red). Empty triangles, filled circles, and broken lines are the PLE spectrum (λ_{obs} = 570 nm), the $\Phi(^1O_2)$ values at photoirradiation of λ_{ex} = 350–550 nm, and photoluminescence spectra (λ_{ex} = 377 and 550 nm) of 10 μM Irbtp–RhB, respectively.

Irbtp–RhB shows high ability for photosensitization of $^1O_2$, with a quantum yield ($\Phi(^1O_2)$) of 43% (λ_{ex} = 365 nm; Abs(365 nm) = 0.17; ESI†, Fig. S2). To identify the $^1O_2$-photosensitizing moiety, $\Phi(^1O_2)$ values were determined with increasing the photoexcitation wavelength (λ_{ex}) from 350 nm to 550 nm, using 1,3-diphenylisobenzofuran[14, 15] and methylene blue[16] as a $^1O_2$ trap and a reference material ($\Phi(^1O_2)$ = 52%), respectively. As shown in Fig. 1b, the action profile (i.e., $\Phi(^1O_2)$ vs λ_{ex}) matches perfectly with the singlet metal-to-ligand charge-transfer (^{1}MLCT) absorption band of Irbtp.[12] On the contrary, direct photoexcitation of the RhB moiety produces smaller quantum yields ($\Phi(^1O_2)$ < 9%), because the triplet

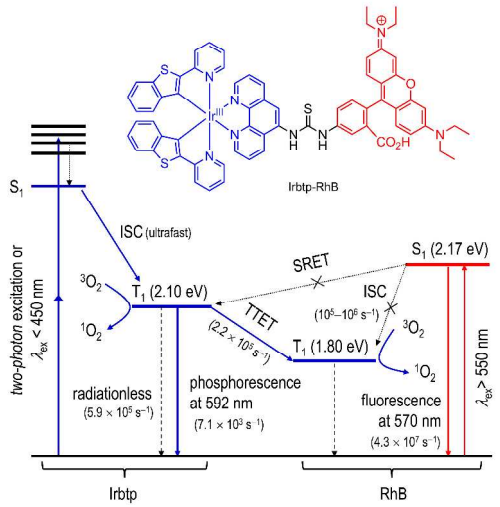

Fig. 2 Proposed mechanism for the photophysical processes of Irbtp–RhB: ISC, intersystem crossing; SRET, spin-restricted energy transfer; TTET, triplet–triplet energy transfer.

state formation in RhB is possible only by triplet–triplet energy transfer from the Irbtp unit at a rate constant, k_{TTET} = 2.2 × 10^5 s^{-1} (ESI†, Fig S1).[17, 18] These results demonstrate that the photoactions of the Irbtp and RhB entities can be performed independently, while intramolecular photoinduced electron transfer from Irbtp to RhB may occur with a positive driving force of 0.56 eV to produce radical ion pair of Irbtp–RhB (i.e., Irbtp$^{\bullet+}$–RhB$^{\bullet-}$; ESI†, Fig. S3). This decoupling nature also affords significant photostability, as demonstrated by the Φ_{PL} and $\Phi(^1O_2)$ values being unaffected by the continuous exposure to a 550 nm beam for 10 min (ESI†, Fig. S4). Taking the results into consideration, a photophysical scheme of Irbtp–RhB is summarized as Fig. 2. It is noteworthy that the unidirectionality in the energy transfer is the key feature that enables the independent actions of fluorescence and $^1O_2$ photosensitization.

Having understood the photophysical mechanism, photobiological utility of Irbtp–RhB was examined. Irbtp–RhB is cell-permeable when a 10 μM stock solution in DMSO is added to the culture medium of live HeLa cells at 37 °C. The intracellular uptake of Irbtp–RhB may mainly involve passive diffusion, because incubation at 4 °C and treatments of the cells with endocytic inhibitors (50 μM chloroquine or 50 mM NH_4Cl)[19] and metabolic inhibitors (50 mM 2-deoxy-D-glucose + 5 μM oligomycin)[20] do not alter the cellular entry (ESI†, Fig. S5). Bright punctate patterns are localized within the lysosomes of the treated HeLa cells, as seen from the fluorescence images obtained through the excitation (λ_{ex} = 488 nm) and emission (λ_{em} = 551–591 nm) channels adjusted for the RhB fluorescence (Fig. 3a; see ESI†, Fig. S6 for more images). Co-staining experiments with 500 nM LysoTracker Red (Molecular Probe) reveal the lysosomal staining capability of Irbtp–RhB (overlap coefficient = 0.99). In addition to the confocal laser-scanning microscopy, Irbtp–RhB is compatible with the standard set-up for fluorescence lifetime imaging microscopy (Fig. 3b).[21]

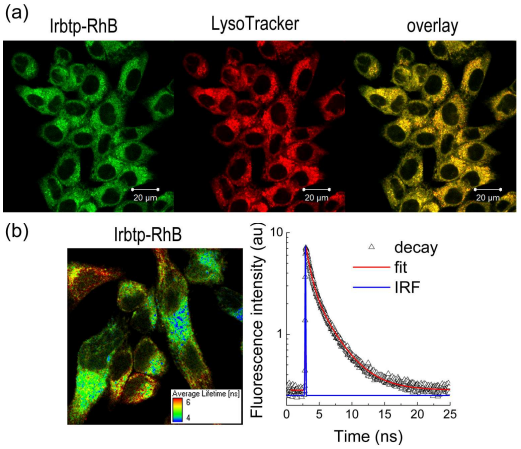

Fig. 3 Lysosomal staining of HeLa cells with Irbtp–RhB. (a) Confocal laser-scanning micrographs of HeLa cells co-stained with 10 μM Irbtp–RhB (10 min incubation at 37 °C) and 500 nM LysoTracker Red (2 h incubation at 37 °C): Left, fluorescence image from Irbtp–RhB (λ_{ex} = 488 nm; λ_{em} = 551–591 nm); middle, fluorescence image from LysoTracker Red (λ_{ex} = 577 nm; λ_{em} = 590–747 nm); right, overlay image. Scale bar = 20 μm. (b) Fluorescence lifetime-imaging micrograph of HeLa cells treated with 10 μM Irbtp–RhB (10 min incubation at 37 °C): Left, lifetime image (250 pixel × 250 pixel and 80 μm × 80 μm) of the cells acquired after picosecond laser excitation at 470 nm (repetition rate = 40 MHz, pulse power = 1 μW, and acquisition window = 5 ms per pixel); right, fluorescence decay traces (black symbols) and their fit (red curve) to a biexponential decay model (τ_{avg} = 3.2 ns). Blue curve is the instrumental response function.

Finally, photoinduced cytotoxicity by intracellular generation of $^1O_2$ has been evaluated. HeLa cells pretreated with different concentrations (0–20 μM, 1 h at 37 °C) of Irbtp–RhB were photoirradiated using a two-photon beam at 800 nm (32 nJ, 80 MHz). The excitation wavelength corresponded to the two-photon absorption of Irbtp, although quantitative evaluations require higher precision of the measurements. Cells that were kept under dark served as controls to estimate dark cytotoxicity of Irbtp–RhB. As shown in Fig. 4a, the 800 nm photoirradiation resulted in vacuolization of the Irbtp–RhB-treated cells. In sharp contrast, neither 561 nm photoirradiation (one-photon) of the treated cells nor 800 nm excitation (two-photon) of untreated cells led to such changes. MTS assays were employed to quantitate the photoinduced cytotoxicity. As shown in Fig. 4b, the 800 nm two-photon photoexcitation significantly reduces the cell viability value < 30% (10 μM Irbtp–RhB, 15 min photoirradiation). The efficacy of phototoxicity, estimated by the cell viability ratio of the control cells over the photoirradiated cells, reaches as high as 2.72 after 15 min photoirradiation.

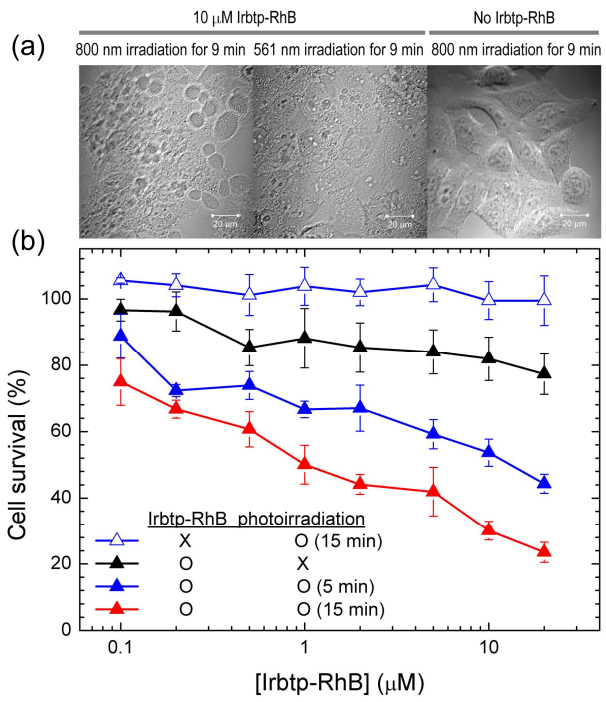

Fig. 4 Photoinduced cell death by Irbtp–RhB. (a) Changes in the cell morphology of HeLa cells under two-photon photoirradiation (80 MHz, 32 nJ) at 800 nm (left and right panels) and one-photon photoirradiation at 561 nm (middle panel). The cells in the left and middle panels were preincubated with 10 μM Irbtp–RhB. See ESI† for the movie clips showing temporal changes of the HeLa cells upon photoirradiation. (b) MTS cell viability data for HeLa cells incubated in the presence and absence of 0.1–20 μM Irbtp–RhB (1 h at 37 °C). The cells were photoirradiated for 5 and 15 min prior to the MTS assay.

To summarize, we synthesized a molecular dyad comprising a biscyclometalated Ir(III) complex and rhodamine B, and characterized its dual functionality for fluorescence imaging and photodynamic therapy. The unidirectional energy transfer and the ability for selective photoexcitation enable independent operation of the lysosomal staining and the photosensitization of $^1O_2$.

This work was supported by the CRI (2-2012-1794-001-1 to W.N.) and GRL (2010-00353 to W.N.) programs from the NRF of Korea.

Notes and references

[a] *Department of Chemistry and Nanoscience, Ewha Womans University, Seoul 120-750, Korea; Fax: +82-2-3277-4441 Tel: +82-2-3277-2392; E-mail: wwnam@ewha.ac.kr (WN).*
[b] *Department of Advanced Materials Engineering for Information and Electronics, Kyung Hee University, Yongin, Gyeonggido 446-701, Korea; Tel: +82-31-201-5273; E-mail: odds2@khu.ac.kr (YY).*

† Electronic Supplementary Information (ESI) available: Experimental details and Fig. S1–S10, plotting photoluminescence decay traces after nanosecond and picosecond laser excitation, determination of $\Phi(^1O_2)$ values, cyclic voltammograms, photostability of Φ_{PL} and $\Phi(^1O_2)$, cellular uptake, subcellular localization of Irbtp–RhB, and copies of ^1H and ^{13}C NMR spectra. See DOI: 10.1039/c000000x/

1. J. P. Celli, B. Q. Spring, I. Rizvi, C. L. Evans, K. S. Samkoe, S. Verma, B. W. Pogue and T. Hasan, *Chem. Rev*., 2010, **110**, 2795-2838.
2. A. Bogaards, A. Varma, K. Zhang, D. Zach, S. K. Bisland, E. H. Moriyama, L. Lilge, P. J. Muller and B. C. Wilson, *Photochem. Photobiol. Sci*., 2005, **4**, 438-442.
3. S. N. Goldberg, C. J. Grassi, J. F. Cardella, J. W. Charboneau, G. D. Dodd, III, D. E. Dupuy, D. Gervais, A. R. Gillams, R. A. Kane, F. T. Lee, Jr., T. Livraghi, J. McGahan, D. A. Phillips, H. Rhim and S. G. Silverman, *Radiology*, 2005, **235**, 728-739.
4. S. S. Kelkar and T. M. Reineke, *Bioconjugate Chem.*, 2011, **22**, 1879-1903.
5. M. R. Gill and J. A. Thomas, *Chem. Soc. Rev.*, 2012, **41**, 3179-3192.
6. C.-T. Poon, P.-S. Chan, C. Man, F.-L. Jiang, R. N. S. Wong, N.-K. Mak, D. W. J. Kwong, S.-W. Tsao and W.-K. Wong, *J. Inorg. Biochem*., 2010, **104**, 62-70.
7. H. Ke, H. Wang, W.-K. Wong, N.-K. Mak, D. W. J. Kwong, K.-L. Wong and H.-L. Tam, *Chem. Commun.*, 2010, **46**, 6678-6680.
8. C. Truillet, F. Lux, J. Moreau, M. Four, L. Sancey, S. Chevreux, G. Boeuf, P. Perriat, C. Frochot, R. Antoine, P. Dugourd, C. Portefaix, C. Hoeffel, M. Barberi-Heyob, C. Terryn, L. v. Gulick, G. Lemercier and O. Tillement, *Dalton Trans*., 2013, **42**, 12410-12420.
9. S. P.-Y. Li, C. T.-S. Lau, M.-W. Louie, Y.-W. Lam, S. H. Cheng and K. K.-W. Lo, *Biomaterials*, 2013, **34**, 7519-7532.
10. A. Nakagawa, Y. Hisamatsu, S. Moromizato, M. Kohno and S. Aoki, *Inorg. Chem.*, 2014, **53**, 409-422.
11. G. Battogtokh, H.-B. Liu, S.-M. Bae, P. K. Chaturvedi, Y.-W. Kim, I.-W. Kim and W. S. Ahn, *J. Porphyr. Phthalocya*., 2012, **16**, 1024-1031.
12. H. Woo, S. Cho, Y. Han, W.-S. Chae, D.-R. Ahn, Y. You and W. Nam, *J. Am. Chem. Soc*., 2013, **135**, 4771–4787.
13. S. P.-Y. Li, T. S.-M. Tang, K. S.-M. Yiu and K. K.-W. Lo, *Chem. Eur. J*., 2012, **18**, 13342-13354.
14. S. Onitsuka, H. Nishino and K. Kurosawa, *Tetrahedron*, 2001, **57**, 6003-6009.
15. J.-M. Aubry, C. Pierlot, J. Rigaudy and R. Schmidt, *Acc. Chem. Res*., 2003, **36**, 668-675.
16. N. Adarsh, R. R. Avirah and D. Ramaiah, *Org. Lett*., 2010, **12**, 5720–5723.
17. C. Ringemann, A. Schönle, A. Giske, C. v. Middendorff, S. W. Hell and C. Eggeling, *ChemPhysChem*, 2008, **9**, 612-624.
18. R. Menzel and E. Thiel, *Chem. Phys. Lett*., 1998, **291**, 237-243.
19. C. Li, M. Yu, Y. Sun, Y. Wu, C. Huang and F. Li, *J. Am. Chem. Soc*., 2011, **133**, 11231-11239.
20. C. A. Puckett and J. K. Barton, *Biochemistry*, 2009, **45**, 11711-11716.
21. M. Y. Berezin and S. Achilefu, *Chem. Rev*., 2010, **110**, 2641-2684.

For ToC Graphic Only